Predicting interfacial tension and adsorption at fluid-fluid interfaces for mixtures of PFAS and/or hydrocarbon surfactants

Bo Guo,*,† Hassan Saleem,† and Mark L. Brusseau†,‡

†*Department of Hydrology and Atmospheric Sciences, University of Arizona, Tucson, Arizona, 85721, United States*

‡*Department of Environmental Science, University of Arizona, Tucson, Arizona, 85719, United States*

E-mail: boguo@arizona.edu

Abstract

Many per- and polyfluoroalkyl substances (PFAS) are surface active and adsorb at fluid–fluid interfaces. The interfacial adsorption controls PFAS transport in multiple environmental systems, including leaching through soils, accumulation in aerosols, and treatment methods such as foam fractionation. Most PFAS contamination sites comprise mixtures of PFAS as well as hydrocarbon surfactants, which complicates their adsorption behaviors. We present a mathematical model to predict interfacial tension and adsorption at fluid–fluid interfaces for multicomponent PFAS and hydrocarbon surfactants. The model is derived from simplifying a prior advanced thermodynamic-based model and applies to nonionic and ionic mixtures of the same charge sign with swamping electrolytes. The only required model input are the single-component Szyszkowski parameters obtained for the individual components. We validate the model using literature interfacial tension data of air–water and NAPL (non-aqueous phase liquid)–water interfaces covering a wide range of multicomponent PFAS and hydrocarbon surfactants. Application of the model to representative porewater PFAS concentrations in the vadose zone suggests competitive adsorption can significantly reduce PFAS retention (up to 7 times) at some highly-contaminated sites. The multicomponent model can be

readily incorporated into transport models to simulate the migration of mixtures of PFAS and/or hydrocarbon surfactants in the environment.

Synopsis Statement: A mathematical model for predicting interfacial tension and fluid–fluid interfacial adsorption for mixtures of PFAS and/or hydrocarbon surfactants. The model is validated by various interfacial tension data from the literature.

Keywords: PFAS, air–water interfacial adsorption, competitive adsorption, surfactant mixture, hydrocarbon surfactants, leaching, thermodynamics.

1 Introduction

PFAS are widespread and have contaminated surface water, soils, sediments, groundwater, and the atmosphere. In particular, vadose zones serve as significant PFAS reservoirs that pose long-term threats for contaminating groundwater[1–8]. The amphiphilic properties of PFAS distinguish their vadose-zone transport behaviors from that of traditional non-surface-active contaminants[9,10]. Adsorption at fluid–fluid interfaces was shown to contribute to PFAS retention in soils by laboratory experiments[11–18], field porewater sampling[19–22], and mathematical modeling studies[10,23–28]. Air-water interfacial adsorption also affects the retention of PFAS by aerosols and the subsequent atmospheric transport[29–31], and the operation of multiple remediation methods such as foam fractionation[32,33] and carbon adsorption.[34,35]

Surface tension (ST) measurement combined with the Gibbs adsorption theory have been used to quantify the adsorption of single-component surfactants at fluid–fluid interfaces over many decades[36]. More recently, they have been applied to describe the adsorption of single-component PFAS at air–water and NAPL–water interfaces[9,12,37–39]. The ST and interfacial tension (IFT) data for single-component PFAS as a function of PFAS concentration are shown to be well described by the Szyszkowski equation. Combining the Gibbs adsorption equation and the Szyszkowski equation leads to the commonly used Langmuir-Szyszkowski isotherm for single-component PFAS adsorption at the fluid–fluid interface[36], which was shown to agree well the retardation analysis of water-unsaturated miscible-displacement experiments[11,15,26,40]. Nevertheless, there is an ongoing debate as to whether the fluid–fluid interfacial adsorption of PFAS at lower concentrations follows the Langmuir-Szyszkowski isotherm or Freundlich isotherm[17,39,41–44]. Settling the debate will require direct experimental evidence of adsorption at lower PFAS concentrations. The present study focuses on multicomponent PFAS and hydrocarbon-surfactant systems, assuming that the Langmuir-Szyszkowski isotherm is valid for describing single-component fluid–fluid interfacial adsorption.

Most PFAS-impacted sites comprise mixtures of PFAS and hydrocarbon surfactants[6,45–47]. The multicomponent PFAS and hydrocarbon surfactants may interact with each other, such as competing for adsorption sites at the fluid–fluid interfaces, which will subsequently influence the reduction of IFT. Mixtures of hydrocarbon surfactants have been widely studied for potential synergistic effects for reducing IFT[36,48]. IFT data of multicomponent PFAS or mixtures of PFAS and hydrocarbon surfactants have also been reported[18,39,49–54], some of which have demonstrated the presence of competitive adsorption among PFAS and hydrocarbon surfactants.

Several studies applied a direct extension of the single-component Langmuir-Szyszkowski isotherm to model the fluid–fluid interfacial adsorption of multicomponent PFAS[18,50,52,53,55]. However, the multicomponent Langmuir isotherm is not thermodynamically consistent unless all components have equal maximum adsorption capacity[56–59], which is not fulfilled for most PFAS and hydrocarbon surfactants. More advanced models have been previously developed for predicting IFT and fluid–fluid interfacial adsorption of hydrocarbon surfactant mixtures[60–62], but these advanced models are less practically useful due to a large number of required model parameters. Simpler models were later developed that significantly reduce the number of model parameters[63–65]. While the simplified models successfully predict the IFT of some hydrocarbon mixtures[63,64], the simplifying assumptions lead to theoretical inconsistencies in predicting multicomponent fluid–fluid interfacial adsorption (see sections 2 and 4). The objective of the present study is to develop and validate a new thermodynamically consistent simplified model that can predict ST/IFT and the fluid–fluid interfacial adsorption of mixtures of PFAS and/or hydrocarbon surfactants using only the single-component Szyszkowski parameters for the individual components.

2 Mathematical model

We derive a thermodynamically consistent simplified model for predicting ST/IFT and fluid–fluid interfacial adsorption of mixtures of PFAS and/or hydrocarbon surfactants using only the single-component Szyszkowski parameters for the individual components. The simplified model is based on a prior advanced mathematical model derived from thermodynamic principles[60,61]. The only assumption involved in our simplification is that intermolecular interactions between surfactants are negligible at fluid–fluid interfaces. Additional details of the advanced model and other information, including the connection and difference between the different simplified models are in sections S1-S2 in the supporting information (SI).

We consider mixtures of nonionic surfactants or ionic surfactants with swamping electrolytes in the solution. In the present study, the ionic surfactants need to have the same

sign of charge. Let γ_0 and γ be the ST/IFT without and with dissolved surfactants in the solution. We define the surface pressure as $\pi = \gamma_0 - \gamma$. Using the subscript i to refer to a PFAS or hydrocarbon surfactant component in the mixture ($i = 1, 2, ..., N$), a_i and b_i are the Szyszkowski parameters for the single-component PFAS or hydrocarbon surfactant (see section S1), and C_i is the aqueous concentration. When intermolecular interactions between surfactants at fluid–fluid interfaces are negligible, the equations for the surface pressure (i.e., surface equation of state) and interfacial adsorption in the advanced model for a mixture of N PFAS or hydrocarbon surfactants (Eqs. S2.1-S2.3 in SI) can be simplified as

$$\pi = -\gamma_0 b \ln\left(1 - \Sigma_{i=1}^{i=N} \hat{\theta}_i\right), \tag{1}$$

$$\frac{C_i}{a_i} = \frac{\hat{\theta}_i}{\left(1 - \Sigma_{i=1}^{i=N} \hat{\theta}_i\right)^{n_i}}. \tag{2}$$

Where $\hat{\theta}_i = \hat{\Gamma}_i \omega_i$ is the monolayer coverage for surfactant component i. $\hat{\Gamma}_i$ is the surface excess and $\omega_i = R_g T/(\gamma_0 b_i)$ is the partial molar surface area, where R_g is the universal gas constant, and T is temperature. Here $\hat{}$ is used to differentiate from the variables when PFAS or hydrocarbon surfactant exists as a single component (see section S1). $b = \Sigma_{i=1}^{i=N} \hat{\theta}_i b_i / \Sigma_{i=1}^{i=N} \hat{\theta}_i$ is the mean of b_i, and $n_i = b/b_i$.

Substituting Eq. (1) to Eq. (2) yields

$$\hat{\theta}_i = \frac{C_i}{a_i} e^{-\frac{\pi}{\gamma_0 b_i}}. \tag{3}$$

Then, substituting $b = \Sigma_{i=1}^{i=N} b_i \frac{C_i}{a_i} e^{-\frac{\pi}{\gamma_0 b_i}} / \Sigma_{i=1}^{i=N} \frac{C_i}{a_i} e^{-\frac{\pi}{\gamma_0 b_i}}$ and Eq. (3) to Eq. (1) gives a surface equation of state for the mixture where the surface pressure π is the only unknown

$$\pi = -\gamma_0 \frac{\Sigma_{i=1}^{i=N} b_i \frac{C_i}{a_i} e^{-\frac{\pi}{\gamma_0 b_i}}}{\Sigma_{i=1}^{i=N} \frac{C_i}{a_i} e^{-\frac{\pi}{\gamma_0 b_i}}} \ln\left(1 - \Sigma_{i=1}^{i=N} \frac{C_i}{a_i} e^{-\frac{\pi}{\gamma_0 b_i}}\right). \tag{4}$$

Eq. (4) is a nonlinear equation that can be solved numerically using an iterative method. After obtaining π, $\hat{\theta}_i$ can then be computed via Eq. (3). Subsequently, the surface excess $\hat{\Gamma}_i$ and the fluid–fluid interfacial adsorption coefficient $\hat{K}_{ia,i}$ in the presence of multicomponent PFAS and hydrocarbon surfactants can be computed as $\hat{\Gamma}_i = \frac{\gamma_0 b_i C_i}{a_i R_g T} e^{-\frac{\pi}{\gamma_0 b_i}}$ and $\hat{K}_{ia,i} = \frac{\gamma_0 b_i}{a_i R_g T} e^{-\frac{\pi}{\gamma_0 b_i}}$. Both $\hat{\Gamma}_i$ and $\hat{K}_{ia,i}$ are nonlinear functions of the concentrations of the surfactant components in the mixture.

Fainerman and Miller[63] also derived a simplified model from the Lucassen-Reynders formulation[60,61] by employing the assumption of negligible intermolecular interactions at

fluid–fluid interfaces. Their simplified model predicts the ST/IFT of several hydrocarbon surfactant mixtures[63,64]. However, two additional assumptions employed in their derivation cause theoretical inconsistency when predicting fluid–fluid interfacial adsorption. When computing b, the interfacial adsorption in the mixture is assumed either proportional to the surface pressure (for extremely dilute surface layers) of the single components or inversely proportional to the partial molar surface area (for a densely packed layer at a sufficiently large surface pressure). Additionally, when deriving the surface equation of state for the surfactant mixture, n_i in Eq. (2) was set to 1 (i.e., $b = b_i$), which indirectly assumes that the maximum adsorption for all components is equal. The theoretical inconsistency of the Fainerman and Miller model[63] (hereafter referred to as FM model) is discussed in more detail in section S2 and also illustrated in an example in section 4. Our simplified model (Eqs. (1-4)) does not involve any of the two additional assumptions and therefore maintains the thermodynamic consistency of the original advanced model[60,61,65].

As discussed briefly in the Introduction, the multicomponent Langmuir model also uses the single-component Szyszkowski parameters for the individual components as input. However, the multicomponent Langmuir model is only thermodynamically consistent when all components have equal maximum adsorption (i.e., $b = b_i$), which is invalid from most PFAS and hydrocarbon surfactants. In section S2, we show that the FM model[63] recovers the multicomponent Langmuir model when $b = b_i$, which suggests that the multicomponent Langmuir model introduces additional errors compared to the FM model when b_i varies among the PFAS and hydrocarbon surfactants. Due to the thermodynamic inconsistency, the multicomponent Langmuir model does not correspond to a thermodynamically consistent surface equation of state for the surface pressure of surfactant mixtures, which is an additional limitation of the multicomponent Langmuir model.

3 Predicted vs. measured surface and interfacial tension data

We validate our simplified multicomponent model presented in section 2 by predicting a series of measured ST/IFT data sets for various PFAS and hydrocarbon surfactant mixtures reported in the literature. The single-component Szyszkowski parameters obtained from the ST/IFT data for the individual components are presented in Table S1. Because all models discussed in the present study do not account for the formation of supramolecular structures above the critical micelle concentrations (CMC), we only examine concentrations below the CMCs in our analyses. The mean squared errors for all ST/IFT predictions are presented

in the SI.

3.1 PFAS mixtures

We collect ST/IFT data sets for PFAS mixtures from four experimental studies[18,39,50,52], all of which can be considered with electrolyte excess (synthetic groundwater or 0.01 M NaCl). Using the single-component Szyszkowski parameters as input, we employ Eq. (4) to predict the ST/IFT in the presence of PFAS mixtures at various mixing ratios. For some data sets, we present the comparisons between our simplified model and the FM model (Eq. S2.5) to illustrate the errors that may be introduced by the additional assumptions employed therein.

We first consider the binary mixtures of PFAS in synthetic groundwater[52], which include four pairs at different mixing ratios. The model predictions and the measured ST agree remarkably well for the binary mixtures of PFDA–PFNA and PFDA–PFOA (Figure 1ab). The agreement for the binary mixtures of PFDA–PFHpA and PFDA–PFPeA is also reasonably good (Figure 1cd), but some deviations are present (see computed errors in Table S2). Possible causes of the deviation are discussed later in this section.

We then test the performance of the model for mixtures with more than two PFAS. These include ternary mixtures and an equimolar mixture of eight PFAS in synthetic groundwater reported by Silva et al.[52], and another equimolar mixture of eight PFAS in 0.01 M NaCl solution reported by Schaefer et al.[39]. Inspection of Figure 2 shows that the model agrees well with the measured multicomponent surface tension data, though the eight-component mixtures see greater deviations (see computed errors in Table S3). Even for the eight-component mixtures, the 95% confidence intervals of the predicted ST values bracket the measured data (see Figure S1). The FM model produces comparable predictions (Figure 2def), which also show greater deviations for the eight-component mixtures.

Lastly, we use a set of IFT data[18] to test the model for PFAS mixtures in a water-NAPL system. The IFT data were collected for a binary equal-mass mixture and an equal-mass mixture of six PFAS. The solution comprised 0.01 M NaCl and the NAPL was tetrachloroethylene (PCE). The predicted and measured IFT data agree well for both the binary and six-component mixtures (Figure 3ab), which demonstrates the efficacy of the model for NAPL–water systems. The predictions by the FM model are also presented for comparison (Figure 3cd). The FM model agrees well with the experimental data for the binary mixture PFNA–PFOS, but it deviates significantly from the measured data for the six-component mixture. This is due to the Szyszkowski parameter b_i for PFNA and PFOS being very close in the binary mixture, but strong variations are present in the Szyszkowski parameter b_i among the six PFAS. In that case, the assumption of equal b_i and the approximations used

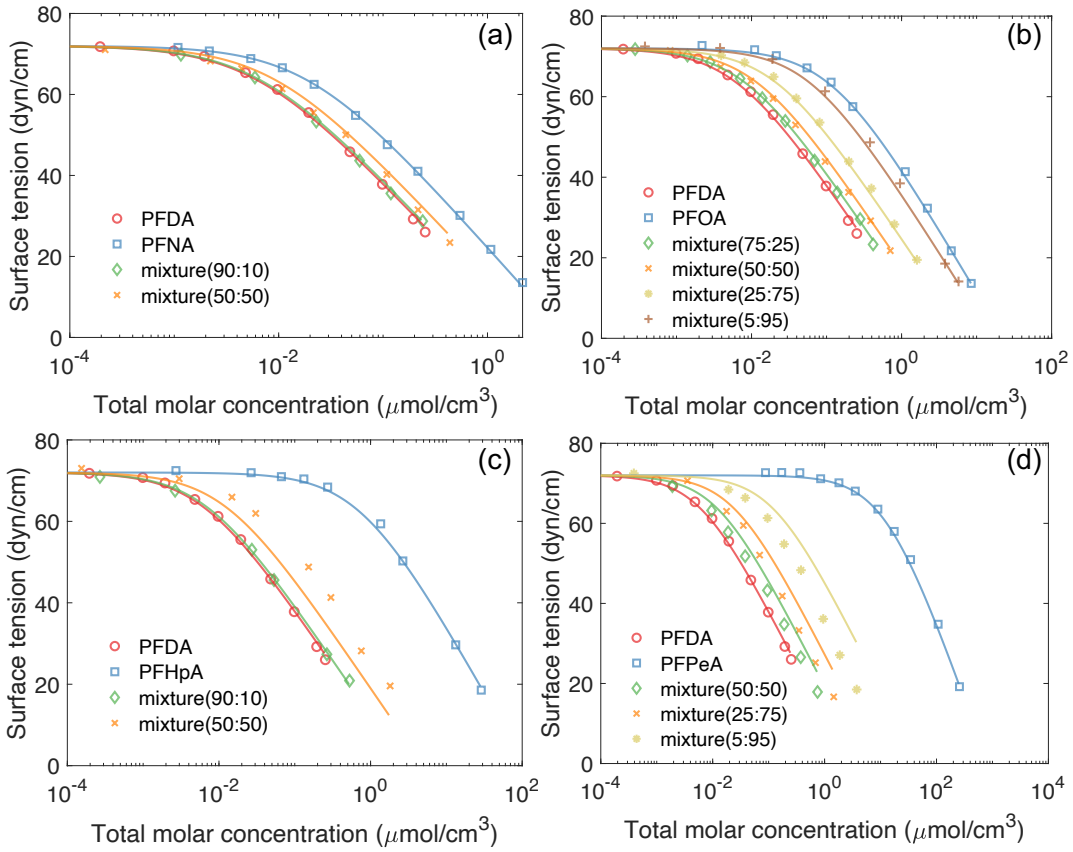

Figure 1: ST data for PFAS and their binary mixtures. (a–d) are for binary mixtures of PFDA–PFNA, PFDA–PFOA, PFDA–PFHpA, and PFDA–PFPeA, respectively. The numbers in the parentheses denote mole ratios. The binary mixtures are predicted by our multicomponent model. For all figures in the present study, the markers denote measured data, and the solid lines for the individual PFAS are fitted by the Szyszkowski equation. The measured data were reported in Silva et al. [52].

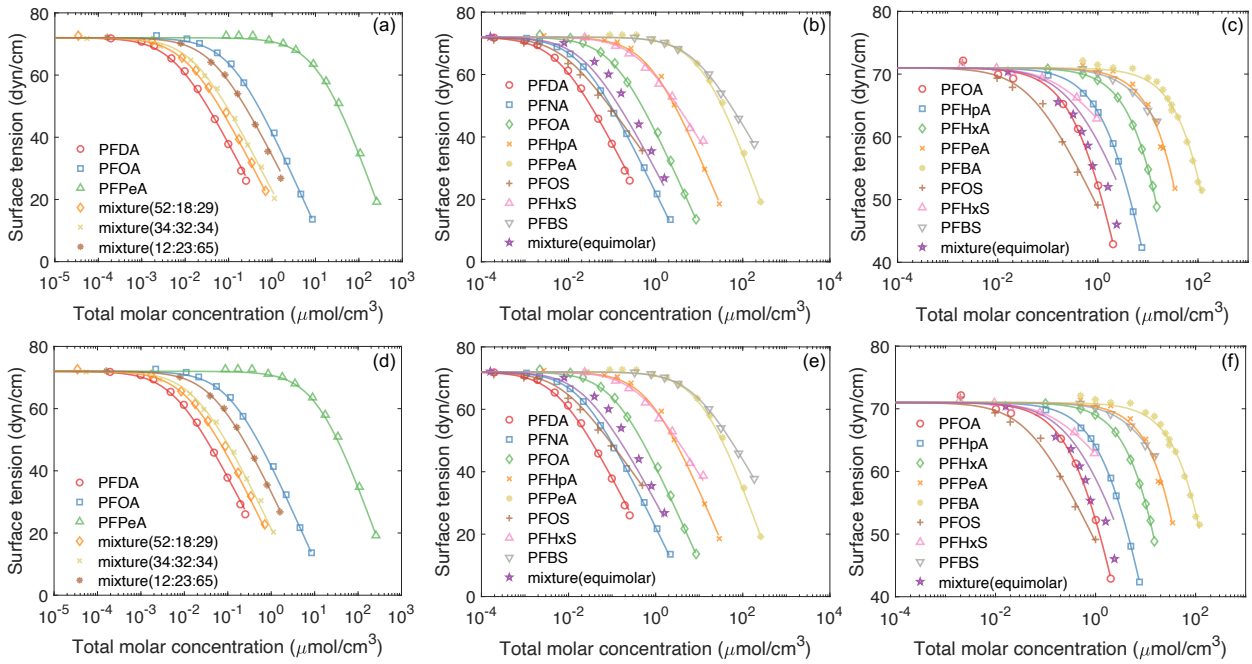

Figure 2: ST data for PFAS and their multicomponent mixtures. The numbers in the parentheses of the ternary mixtures denote mole ratios. Predictions by our multicomponent model (a–c) and the FM model[64] (d–f) are presented for comparison. The measured data of the first two columns (a, b, d, e) were reported in Silva et al.[52], and those in the third column (c and f) were reported in Schaefer et al.[39].

to obtain b in the FM model introduces errors in the predicted IFT values.

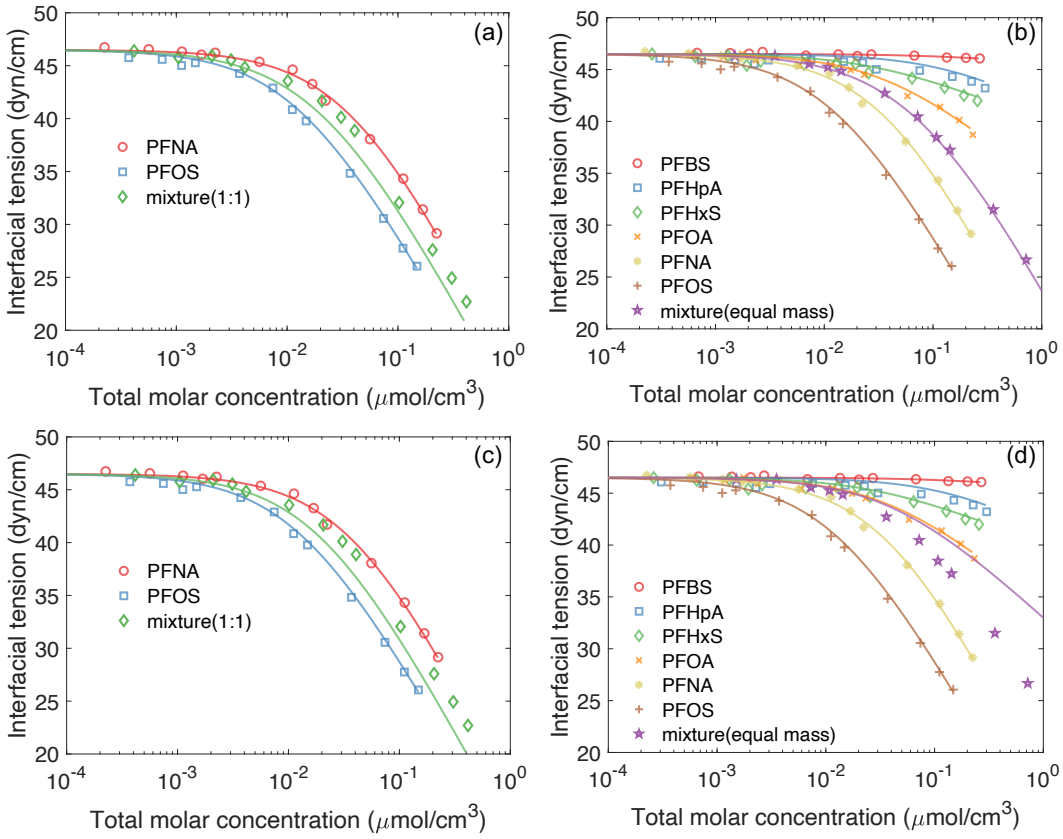

Figure 3: IFT data between water and a NAPL (i.e., PCE) for PFAS and their mixtures. Predictions by our multicomponent model (a–b) and the FM model[64] (c–d) are presented for comparison. The measured data were reported in Liao et al.[18].

All PFAS in the measured data sets discussed above were purchased from Sigma-Aldrich Co. and used without further purification. The impurities of the PFAS from Sigma-Aldrich Co. vary among different PFAS, but they are usually a few percent. For example, the purities for PFPeA, PFHpA, PFOA, PFNA, and PFDA are 97%, 99%, 96%, 97%, and 95%, respectively[38,52]. The compositions of the impurities in these PFAS remain unknown. We hypothesize that the presence of surface-active impurities caused the deviations observed for the two binary pairs with a short-chain PFAS (PFHpA and PFPeA; Figure 1cd). This is consistent with the observation that the deviation becomes greater as the concentration of the short-chain PFAS increases—surface-active impurities in the solution will have a greater impact on the IFT of the mixture as the concentration of the long-chain PFAS decreases and becomes less important in the mixture. However, the specific impurities in the PFAS products need to be characterized and quantified to further test the hypothesis.

3.2 PFAS and hydrocarbon surfactant mixtures

We use the ST/IFT data sets from Ji et al.[53] and Zhao et al.[49] to further validate our simplified multicomponent model for predicting the ST/IFT for mixtures of PFAS and a hydrocarbon surfactant. All data sets can be considered to have electrolyte excess.

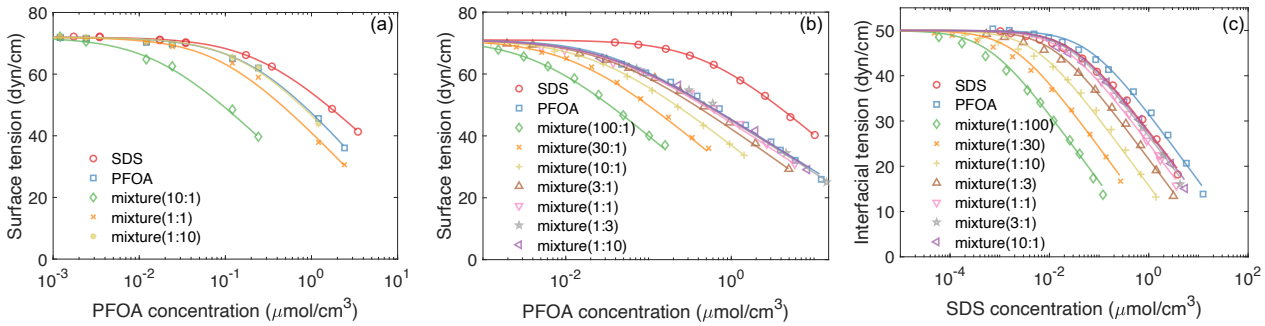

Figure 4: (a–b) ST data and (c) IFT data between water and n-Heptane for PFOA, SDS, and their binary mixtures. The numbers in the parentheses of the binary mixtures denote mass ratios in (a) and mole ratios in (b–c). The binary mixtures are predicted by our multicomponent model. The measured data in (a) were reported in Ji et al.[53], and those in (b–c) were reported in Zhao et al.[49].

The ST data reported by Ji et al.[53] were for binary mixtures of PFOA and SDS measured in 0.01 M NaCl solution at three mixing ratios of mass concentrations. The PFOA (95% purity) and SDS (98% purity) were purchased from Sigma-Aldrich Co and used without further purification. Figure 4 shows that the model predictions and experimental data agree well for all three mixing ratios. The good agreement between model predictions and measured data implies that the impurities in PFOA and SDS do not play a major role in influencing the ST of the solution of their mixture, likely because impurities are less surface-active compared to PFOA and SDS.

Zhao et al.[49] reported both ST and IFT (between water and n-Heptane) for binary mixtures of PFOA and SDS. The PFOA and SDS were both further purified before use. Comparisons between model predictions and measured IFT data for binary mixtures of PFOA and SDS at constant molar ratios are shown in Figure 4bc (b and c present ST and IFT, respectively). Similar comparisons for binary mixtures of PFOA and SDS with one of their concentrations fixed are presented in Figure 5. We also present the predictions by the FM model (Figure 5cd), which have greater errors for the ST data (Figure 5c), but are very close to our simplified model for the IFT data (Figure 5d). This is expected because the single-component Szyszkowski parameter b_i of PFOA and SDS are greater for the ST data, but they are almost identical for the IFT data (Table S1). For the latter, errors caused by the assumption of equal b_i in the FM model are almost negligible.

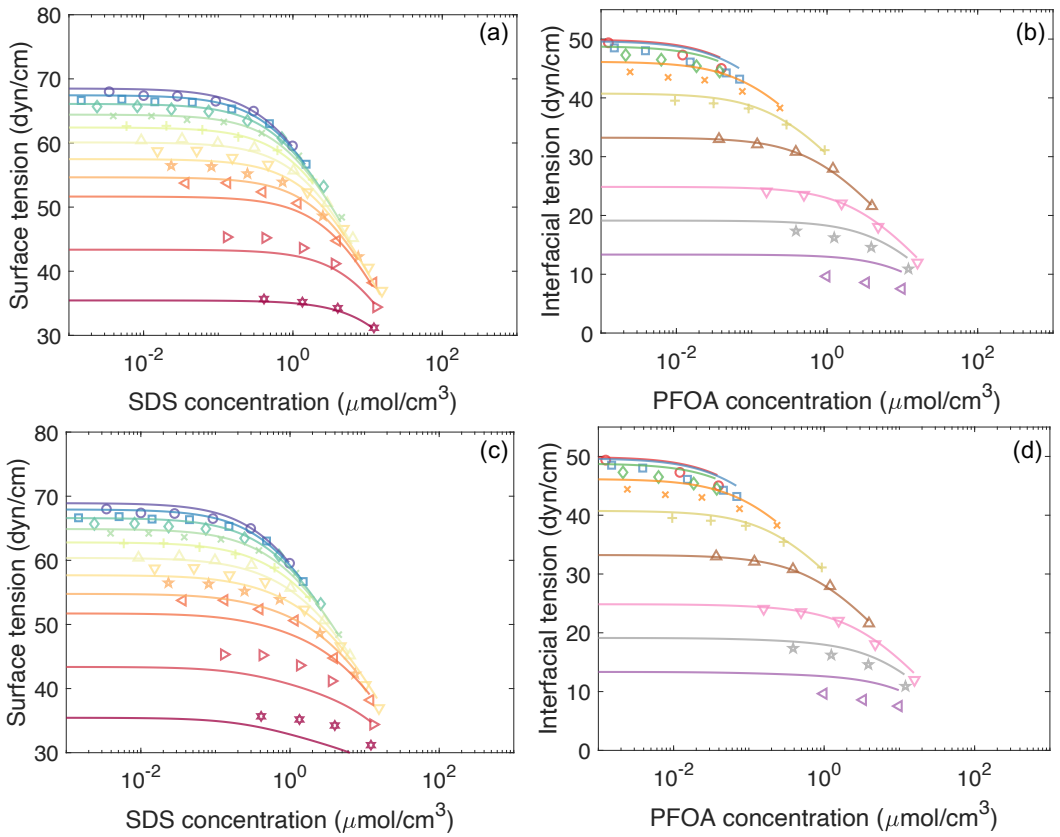

Figure 5: (a, c) ST data and (b, d) IFT data between water and n-Heptane for PFOA and SDS binary mixtures. Our multicomponent model (a–b) and the FM model[64]) are presented for comparison (c–d). From top to bottom, the PFOA concentrations (a and c) are $10^{-2}, 10^{-1.8}, 10^{-1.6}, 10^{-1.4}, 10^{-1.2}, 10^{-1}, 10^{-0.8}, 10^{-0.6}, 10^{-0.4}, 10^{0.12}, 10^{0.6}$ and the SDS concentrations (b and d) are $10^{-3.4}, 10^{-2.8}, 10^{-2.2}, 10^{-1.6}, 10^{-1}, 10^{-0.4}, 10^{0.2}, 10^{0.6}, 10^{1}$. The units are all μmol/cm^3. The measured data were reported in Zhao et al.[49].

Finally, it is important to point out that the main limitation of the FM model is not its prediction of the ST/IFT of the mixture. As discussed above, the FM model gives reasonable predictions of the ST/IFT for PFAS and hydrocarbon mixtures, though they introduce greater errors in some cases. Rather, the major limitation of the FM model lies in its prediction of the fluid-fluid interfacial adsorption. As elaborated in section S2, the fluid-fluid interfacial adsorption predicted by the FM model can lead to theoretically inconsistent results when significant variations are present among the maximum adsorption capacities of the components in the mixture. This limitation is illustrated in the examples presented in section 4.

4 Predicted air–water interfacial adsorption of PFAS and hydrocarbon surfactant mixtures

We employ our simplified multicomponent model to predict the adsorption of PFAS and hydrocarbon surfactants at air–water interfaces. To illustrate the impact of competitive air–water interfacial adsorption on PFAS retention, we consider three scenarios relevant to PFAS retention in the vadose zone beneath a fire training area site impacted by aqueous film forming foam (AFFF). Scenario #1 uses PFAS concentration from a 1% AFFF concentrate diluted at 1:100[4]. Scenarios #2 and #3 consider *in-situ* PFAS porewater concentrations collected by suction lysimeters installed at two AFFF-impacted sites[20,21]. The porewater concentrations reported by Anderson et al.[21] are generally much greater than those from Schaefer et al.[20]. Therefore, the two data sets provide examples of relatively high and low porewater concentrations at AFFF-impacted sites. To simplify the analysis, we selected the greatest porewater concentrations collected by multiple lysimeters at different times reported in these two studies. Based on the availability of porewater concentration data, we consider five PFAS, i.e., PFOS, PFOA, PFHxS, PFHxA, and PFBS. Additionally, we hypothetically consider the presence of a hydrocarbon surfactant given that hydrocarbon surfactants were commonly used in AFFFs[45,66]. SDS is used as an example hydrocarbon surfactant in our analysis. Previous studies reported that hydrocarbon surfactants account for more than 5 times of the PFAS mass in AFFFs[45,66]. We assume that SDS has a concentration that is 5 times of the PFAS with the greatest concentration in soil porewater.

The porewater concentrations for the three scenarios are compiled in Table S7. We assume the soil porewater has a composition similar to synthetic groundwater and obtain the Szyszkowski parameters using the single-component ST data reported in the literature[38,52]. The porewater in soils can be considered to have electrolyte excess. No ST data for SDS

is available under the same synthetic groundwater condition. We approximate it using the Szyszkowski parameters fitted to the ST data from Ji et al. [53] measured in 0.01 NaCl solution. To examine the impact of competitive adsorption, we also compute the air–water interfacial adsorption coefficients of PFAS and SDS when they are present as a single component in the solution using the single-component Langmuir-Szyszkowski model (Eq. S1.4). For comparison, we also present the air–water interfacial adsorption coefficient predicted by the multicomponent Langmuir model (Eq. S2.4) and the FM model (Eq. S2.6). The predicted air–water interfacial coefficients are presented in Table S7.

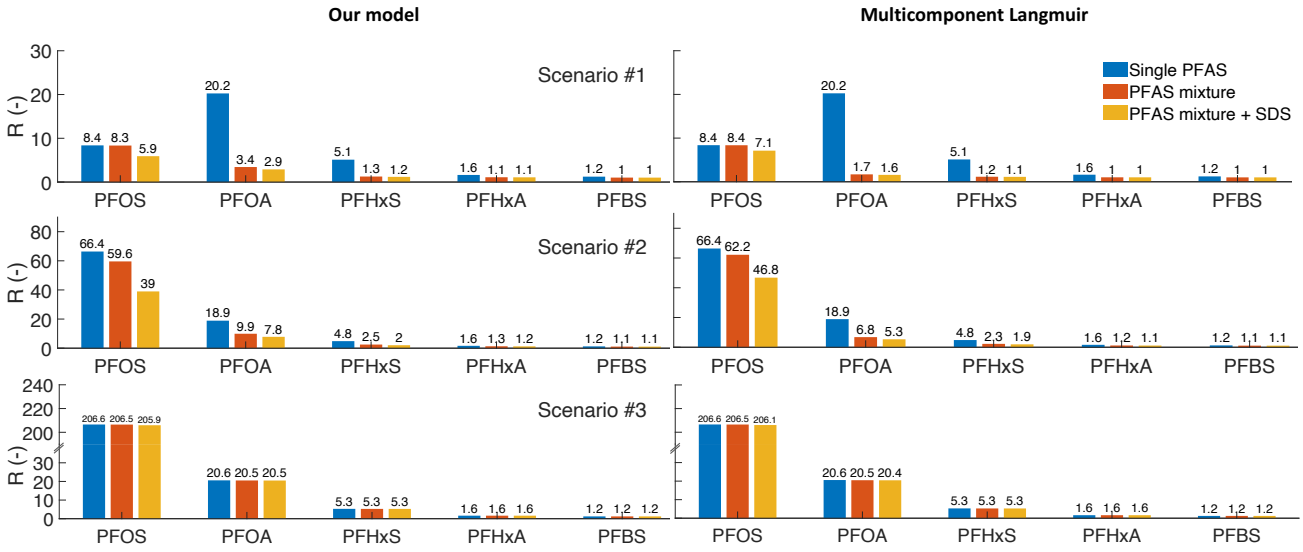

Figure 6: Predicted retardation factors for PFAS mixtures in a water-unsaturated soil with and without the presence of a hydrocarbon surfactant (i.e., SDS). The left and right panels are predictions from our multicomponent and the multicomponent Langmuir model, respectively. The three rows represent retardation factors computed for the porewater concentrations of scenarios 1–3 (Table S7), respectively.

Comparisons between the single-component K_{ia} and the multicomponent K_{ia} predicted by our simplified multicomponent model show that competitive adsorption significantly reduces K_{ia} for all PFAS and SDS in scenarios #1 and #2, but not in scenario #3. In scenario #1, the multicomponent K_{ia} for PFOS and SDS (the two most surface-active components) are approximately 40% and 64% smaller than their single-component K_{ia}. The reduction of K_{ia} due to competitive adsorption is much greater for the four less surface-active PFAS (PFOA, PFHxS, PFHxA, PFBS), wherein their K_{ia} decreases by approximately 8 to 25 times when the five PFAS and SDS are present as mixtures. A similar trend can be observed for scenario #2, though the reduction in K_{ia} is smaller due to the lower porewater concentrations of the most surface-active components PFOS and SDS compared to scenario #1. The K_{ia} for the PFOS and SDS in the mixture are approximately 46% and 40% smaller

than their single-component K_{ia}. The K_{ia} for the four less surface-active PFAS decrease by approximately 3 to 4 times when in the mixture. Conversely, the K_{ia} are almost the same as the single-component K_{ia} for all PFAS and SDS in scenario #3, indicating a minimal impact from competitive adsorption at air–water interfaces. This is because the porewater concentrations in scenario #3 are several orders of magnitude lower than those from scenarios #1 and #2, and as a result, the PFAS and SDS components do not affect each other's adsorption capacity at the air–water interface.

To quantify the impact of competitive adsorption on PFAS retention, we compute the retardation factors for the five PFAS at the given porewater concentrations under representative conditions in the vadose zone. For illustrative purposes, we select a well-characterized soil (i.e., Vinton soil) collected locally in Tucson, Arizona. The hydraulic properties and air–water interfacial area for the Vinton soil measured at different water saturations by various methods were reported in prior studies[67–69]. Here we assume the soil in the vadose zone has a capillary pressure of 75 cm (water content $\theta_w = 0.15$). Using the second-degree polynomial function of water saturation fitted to the air–water interfacial area data measured by aqueous interfacial tracers for the Vinton soil[10], we obtain a specific air–water interfacial area $A_{aw} = 667.5$ cm^2/cm^3. To focus on the impact of air–water interfacial adsorption, here we neglect the retention due to solid-phase adsorption and compute the retardation factor for each PFAS as $R = 1 + K_{ia}A_{aw}/\theta_w$. Substituting K_{ia} computed from the single-component Langmuir-Szyszkowski model, our simplified multicomponent model, and the multicomponent Langmuir model gives retardation factors corresponding to these three models. We also present the retardation factors using both the multicomponent K_{ia} with and without accounting for the presence of SDS. Note that K_{ia} is a nonlinear function of PFAS and SDS concentrations in all models, and the computed R herein represents the retardation at the given porewater concentrations in Table S7.

The comparisons of the retardation factors (Figure 6) are generally consistent with the air–water interfacial adsorption coefficients. Competitive adsorption among PFAS appears to have a significant impact on PFAS retention in the vadose zone in scenarios #1 and 2, but not in #3. For scenarios #1 and #2, the retardation factors for the intermediate surface-active PFAS (PFOA and PFHxS) decrease by approximately 2 to 7 times. The retardation factors for PFOS appear to be less affected. This is because PFOS is the most surface-active component such that its adsorption is minimally influenced by the other PFAS. However, PFOS retention is significantly reduced when SDS is present because SDS has a similar surface activity and is at a relatively large concentration. Similarly, the retention of PFOA and PFHxS is further reduced in the presence of SDS. Interestingly, competitive adsorption appears to have a minor impact on the retention of PFHxA and PFBS. A closer

inspection reveals that air–water interfacial adsorption is much weaker for these two PFAS; their retardation factors are close to 1 even when they are present as single components. Therefore, while competitive adsorption further reduces air–water interfacial adsorption, the reduction in the retardation factor is minimal.

Finally, we discuss the difference between the predicted K_{ia} and retardation factors from our multicomponent model, the multicomponent Langmuir model, and the FM model. The comparisons in Table S7 and Figure 6 show that the multicomponent Langmuir model consistently underestimates the K_{ia} and retardation factors for the less surface-active PFAS, while it overestimates the K_{ia} and retardation factors for the most surface-active PFOS. Though the Szyszkowski parameter b_i only varies moderately among the different PFAS (i.e., b_i is between 0.12 and 0.21), the K_{ia} predicted by the multicomponent Langmuir model can deviate as much as 70% (PFOA in scenario #1) from that computed by our multicomponent model. These results illustrate that the multicomponent Langmuir model can introduce rather significant errors when predicting the retention of PFAS mixtures in the vadose zone. We have also computed the K_{ia} and retardation factors using the FM model (see Table S7 and Figure S2). The FM model sees similar deviations from our multicomponent model. Notably, the FM model produces multicomponent K_{ia} greater than the single-component K_{ia} for some PFAS (i.e., the most surface-active component PFOS in scenario #1), which is theoretically inconsistent for a mixture of anionic PFAS and SDS where no synergistic behaviors are expected. This inconsistency is caused by the two additional assumptions employed when deriving the model formulations as discussed in sections 2 and S2.

5 Environmental implications

We present a mathematical model for predicting ST/IFT and fluid–fluid interfacial adsorption for mixtures of PFAS and/or hydrocarbon surfactants. The model applies to PFAS-only mixtures, hydrocarbon-surfactant-only mixtures, or mixtures of both. The PFAS and hydrocarbon surfactants can be nonionic and ionic (with the same charge sign, i.e., either all anionic or all cationic) with swamping electrolytes. Szyszkowski parameters from the single-component ST/IFT data of individual PFAS or hydrocarbon surfactant are the only required input. Independent model predictions of ST/IFT without any parameter fitting are validated by measured data for a wide range of mixtures of PFAS and hydrocarbon surfactants reported in the literature. The model predictions agree well with the experimental data.

We have employed the multicomponent model to analyze the impact of potential competitive adsorption on PFAS retention in the vadose zone using three representative scenarios of

porewater concentrations including PFAS concentrations in 1% diluted AFFF solution and in *in-situ* porewater collected by suction lysimeters at AFFF-impacted sites. The analyses suggest that competitive adsorption among PFAS at the air–water interfaces may significantly reduce PFAS retention (up to 7 times) in highly contaminated vadose zones. Conversely, our study implies that competitive adsorption is likely minimum at the secondary contamination sites such as agricultural lands contaminated by PFAS-containing biosolids where PFAS concentrations are often orders of magnitude smaller than that of the AFFF-impacted sites[6]. The results also suggest that hydrocarbon surfactants can compete for adsorption sites with PFAS at the air–water interfaces and subsequently reduce PFAS retention. If the hydrocarbon surfactants have not been degraded at the PFAS contamination sites, they should be characterized and accounted for when predicting PFAS transport. Due to its thermodynamic inconsistency, the commonly used multicomponent Langmuir model deviates from our multicomponent model. We also showed that the other commonly used simplified multicomponent model by Fainerman and Miller[63,64] can introduce theoretical inconsistency when applied to model multicomponent fluid-fluid interfacial adsorption.

Our study has significant potential implications concerning the characterization and modeling of PFAS leaching and mass discharge to groundwater for many sites. For example, competitive air–water interfacial adsorption may be one of several factors contributing to the observation of groundwater contamination beneath deep vadose zones at highly contaminated sites. Finally, we note that the validation tests reported herein were conducted using available data sets, all of which comprised ST/IFT data for anionic PFAS and SDS. Additional datasets are needed to test model performance for other PFAS and hydrocarbon surfactant types and under a broader range of conditions, e.g., in the presence of other non-surfactant surface active constituents such as dissolved organic matter. In addition, while our multicomponent model is thermodynamically consistent and has been validated by various ST/IFT data, further validation using direct observations (such as neutron reflectometry) is required to test its efficacy for predicting fluid–fluid interfacial adsorption of mixtures of PFAS and/or hydrocarbon surfactants.

Supporting Information. Formulations for the single-component and advanced multicomponent models. Comments on the different simplified models. Szyskowski parameters for the single-component literature ST/IFT data sets. Errors of predicted ST/IF in Figures 1-5. Predicted air-water interfacial adsorption coefficients from the single-component and different multicomponent models. Figure for predicted ST for the eight-component mixtures with confidence intervals. Figure for predicted retardation factors from our multicomponent model and the FM model.

Acknowledgement

This work was in part supported by the National Science Foundation (2023351 and 2054575) and the Environmental Security Technology Certification Program (Project ER21-5041). Views, opinions, and/or findings contained in this paper are those of the authors and should not be construed as an official Department of Defense position or decision unless so designated by other official documentation. We thank the reviewers for their constructive comments.

References

(1) Xiao, F.; Simcik, M. F.; Halbach, T. R.; Gulliver, J. S. Perfluorooctane sulfonate (PFOS) and perfluorooctanoate (PFOA) in soils and groundwater of a US metropolitan area: migration and implications for human exposure. *Water Research* **2015**, *72*, 64–74.

(2) Weber, A. K.; Barber, L. B.; LeBlanc, D. R.; Sunderland, E. M.; Vecitis, C. D. Geochemical and hydrologic factors controlling subsurface transport of poly-and perfluoroalkyl substances, Cape Cod, Massachusetts. *Environmental Science & Technology* **2017**, *51*, 4269–4279.

(3) Dauchy, X.; Boiteux, V.; Colin, A.; Hémard, J.; Bach, C.; Rosin, C.; Munoz, J.-F. Deep seepage of per-and polyfluoroalkyl substances through the soil of a firefighter training site and subsequent groundwater contamination. *Chemosphere* **2019**, *214*, 729–737.

(4) Høisæter, Å.; Pfaff, A.; Breedveld, G. D. Leaching and transport of PFAS from aqueous film-forming foam (AFFF) in the unsaturated soil at a firefighting training facility under cold climatic conditions. *Journal of Contaminant Hydrology* **2019**, *222*, 112–122.

(5) Anderson, R. H.; Adamson, D. T.; Stroo, H. F. Partitioning of poly-and perfluoroalkyl substances from soil to groundwater within aqueous film-forming foam source zones. *Journal of Contaminant Hydrology* **2019**, *220*, 59–65.

(6) Brusseau, M. L.; Anderson, R. H.; Guo, B. PFAS concentrations in soils: Background levels versus contaminated sites. *Science of the Total environment* **2020**, *740*, 140017.

(7) Adamson, D. T.; Nickerson, A.; Kulkarni, P. R.; Higgins, C. P.; Popovic, J.; Field, J.; Rodowa, A.; Newell, C.; DeBlanc, P.; Kornuc, J. J. Mass-Based, Field-Scale Demonstration of PFAS Retention within AFFF-Associated Source Areas. *Environmental Science & Technology* **2020**, *54*, 15768–15777.

(8) Cáñez, T. T.; Guo, B.; McIntosh, J. C.; Brusseau, M. L. Perfluoroalkyl and Polyfluoroalkyl substances (PFAS) in Groundwater at a Reclaimed Water Recharge Facility. *Science of The Total Environment* **2021**, 147906.

(9) Brusseau, M. L. Assessing the potential contributions of additional retention processes to PFAS retardation in the subsurface. *Science of the Total Environment* **2018**, *613*, 176–185.

(10) Guo, B.; Zeng, J.; Brusseau, M. L. A Mathematical Model for the Release, Transport, and Retention of Per-and Polyfluoroalkyl Substances (PFAS) in the Vadose Zone. *Water Resources Research* **2020**, *56*, e2019WR026667.

(11) Lyu, Y.; Brusseau, M. L.; Chen, W.; Yan, N.; Fu, X.; Lin, X. Adsorption of PFOA at the air–Water interface during transport in unsaturated porous media. *Environmental Science & Technology* **2018**, *52*, 7745–7753.

(12) Brusseau, M. L.; Yan, N.; Van Glubt, S.; Wang, Y.; Chen, W.; Lyu, Y.; Dungan, B.; Carroll, K. C.; Holguin, F. O. Comprehensive retention model for PFAS transport in subsurface systems. *Water Research* **2019**, *148*, 41–50.

(13) Lyu, X.; Liu, X.; Sun, Y.; Gao, B.; Ji, R.; Wu, J.; Xue, Y. Importance of surface roughness on perfluorooctanoic acid (PFOA) transport in unsaturated porous media. *Environmental Pollution* **2020**, *266*, 115343.

(14) Li, Z.; Lyu, X.; Gao, B.; Xu, H.; Wu, J.; Sun, Y. Effects of ionic strength and cation type on the transport of perfluorooctanoic acid (PFOA) in unsaturated sand porous media. *Journal of Hazardous Materials* **2021**, *403*, 123688.

(15) Brusseau, M. L.; Guo, B.; Huang, D.; Yan, N.; Lyu, Y. Ideal versus Nonideal Transport of PFAS in Unsaturated Porous Media. *Water Research* **2021**, 117405.

(16) Van Glubt, S.; Brusseau, M. L. Contribution of nonaqueous-phase liquids to the retention and transport of per and polyfluoroalkyl substances (PFAS) in porous media. *Environmental science & technology* **2021**, *55*, 3706–3715.

(17) Stults, J. F.; Choi, Y. J.; Schaefer, C. E.; Illangasekare, T. H.; Higgins, C. P. Estimation of Transport Parameters of Perfluoroalkyl Acids (PFAAs) in Unsaturated Porous Media: Critical Experimental and Modeling Improvements. *Environmental Science & Technology* **2022**, *56*, 7963–7975.

(18) Liao, S.; Arshadi, M.; Woodcock, M. J.; Saleeba, Z. S.; Pinchbeck, D.; Liu, C.; Cápiro, N. L.; Abriola, L. M.; Pennell, K. D. Influence of Residual Nonaqueous-Phase Liquids (NAPLs) on the Transport and Retention of Perfluoroalkyl Substances. *Environmental Science & Technology* **2022**, *56*, 7976–7985.

(19) Quinnan, J.; Rossi, M.; Curry, P.; Lupo, M.; Miller, M.; Korb, H.; Orth, C.; Hasbrouck, K. Application of PFAS-mobile lab to support adaptive characterization and flux-based conceptual site models at AFFF releases. *Remediation Journal* **2021**, *31*, 7–26.

(20) Schaefer, C. E.; Lavorgna, G. M.; Lippincott, D. R.; Nguyen, D.; Christie, E.; Shea, S.; O'Hare, S.; Lemes, M. C.; Higgins, C. P.; Field, J. A field study to assess the role of air-water interfacial sorption on PFAS leaching in an AFFF source area. *Journal of Contaminant Hydrology* **2022**, *248*, 104001.

(21) Anderson, R. H.; Field, J. B.; DieffenbachCarle, H.; Elsharnouby, O.; Krebs, R. K. Assessment of PFAS in collocated soil and porewater samples at an AFFF-impacted source zone: Field-scale validation of suction lysimeters. *Chemosphere* **2022**, 136247.

(22) Brusseau, M.; Guo, B. PFAS concentrations in soil versus soil porewater: Mass distributions and the impact of adsorption at air-water interfaces. *Chemosphere* **2022**, 134938.

(23) Silva, J. A. K.; Simunek, J.; McCray, J. E. A modified HYDRUS model for simulating PFAS transport in the vadose zone. *Water* **2020**, *12*, 2758.

(24) Zeng, J.; Brusseau, M. L.; Guo, B. Model validation and analyses of parameter sensitivity and uncertainty for modeling long-term retention and leaching of PFAS in the vadose zone. *Journal of Hydrology* **2021**, *603*, 127172.

(25) Zeng, J.; Guo, B. Multidimensional simulation of PFAS transport and leaching in the vadose zone: Impact of surfactant-induced flow and subsurface heterogeneities. *Advances in Water Resources* **2021**, *155*, 104015.

(26) Guo, B.; Zeng, J.; Brusseau, M. L.; Zhang, Y. A screening model for quantifying PFAS leaching in the vadose zone and mass discharge to groundwater. *Advances in Water Resources* **2022**, *160*, 104102.

(27) Wallis, I.; Hutson, J.; Davis, G.; Kookana, R.; Rayner, J.; Prommer, H. Model-based identification of vadose zone controls on PFAS mobility under semi-arid climate conditions. *Water Research* **2022**, *225*, 119096.

(28) Gnesda, W. R.; Draxler, E. F.; Tinjum, J.; Zahasky, C. Adsorption of PFAAs in the Vadose Zone and Implications for Long-Term Groundwater Contamination. *Environmental Science & Technology* **2022**, *56*, 16748–16758.

(29) Johansson, J. H.; Salter, M. E.; Navarro, J. A.; Leck, C.; Nilsson, E. D.; Cousins, I. T. Global transport of perfluoroalkyl acids via sea spray aerosol. *Environmental Science: Processes & Impacts* **2019**, *21*, 635–649.

(30) Sha, B.; Johansson, J. H.; Benskin, J. P.; Cousins, I. T.; Salter, M. E. Influence of water concentrations of perfluoroalkyl acids (PFAAs) on their size-resolved enrichment in nascent sea spray aerosols. *Environmental Science & Technology* **2021**, *55*, 9489–9497.

(31) Sha, B.; Johansson, J. H.; Tunved, P.; Bohlin-Nizzetto, P.; Cousins, I. T.; Salter, M. E. Sea spray aerosol (SSA) as a source of perfluoroalkyl acids (PFAAs) to the atmosphere: field evidence from long-term air monitoring. *Environmental Science & Technology* **2021**, *56*, 228–238.

(32) Burns, D. J.; Stevenson, P.; Murphy, P. J. PFAS removal from groundwaters using Surface-Active Foam Fractionation. *Remediation Journal* **2021**, *31*, 19–33.

(33) Smith, S. J.; Wiberg, K.; McCleaf, P.; Ahrens, L. pilot-scale continuous foam fractionation for the removal of per-and polyfluoroalkyl substances (PFAS) from landfill leachate. *ACS Es&t Water* **2022**, *2*, 841–851.

(34) Meng, P.; Deng, S.; Lu, X.; Du, Z.; Wang, B.; Huang, J.; Wang, Y.; Yu, G.; Xing, B. Role of air bubbles overlooked in the adsorption of perfluorooctanesulfonate on hydrophobic carbonaceous adsorbents. *Environmental science & technology* **2014**, *48*, 13785–13792.

(35) Jiang, X.; Wang, W.; Yu, G.; Deng, S. Contribution of nanobubbles for PFAS adsorption on graphene and OH-and NH2-functionalized graphene: Comparing simulations with experimental results. *Environmental Science & Technology* **2021**, *55*, 13254–13263.

(36) Rosen, M. J.; Kunjappu, J. T. *Surfactants and interfacial phenomena (pp. 66-115)*; John Wiley & Sons, 2012.

(37) Costanza, J.; Arshadi, M.; Abriola, L. M.; Pennell, K. D. Accumulation of PFOA and PFOS at the Air–Water Interface. *Environmental Science & Technology Letters* **2019**, *6*, 487–491.

(38) Silva, J. A.; Martin, W. A.; Johnson, J. L.; McCray, J. E. Evaluating air-water and NAPL-water interfacial adsorption and retention of Perfluorocarboxylic acids within the Vadose zone. *Journal of Contaminant Hydrology* **2019**, *223*, 103472.

(39) Schaefer, C. E.; Culina, V.; Nguyen, D.; Field, J. Uptake of poly-and perfluoroalkyl substances at the air–water interface. *Environmental Science & Technology* **2019**, *53*, 12442–12448.

(40) Brusseau, M. L. Simulating PFAS transport influenced by rate-limited multi-process retention. *Water Research* **2020**, *168*, 115179.

(41) Schaefer, C. E.; Nguyen, D.; Field, J. Response to the Comment on "Uptake of Poly- and Perfluoroalkyl Substances at the Air-Water Interface". *Environmental Science & Technology* **2020**, *54*, 7021–7022.

(42) Arshadi, M.; Costanza, J.; Abriola, L. M.; Pennell, K. D. Comment on "Uptake of Poly- and Perfluoroalkyl Substances at the Air–Water Interface". *Environmental Science & Technology* **2020**, *54*, 7019–7020.

(43) Brusseau, M. L. Examining the robustness and concentration dependency of PFAS air-water and NAPL-water interfacial adsorption coefficients. *Water Research* **2021**, *190*, 116778.

(44) Le, S.-T.; Gao, Y.; Kibbey, T. C.; Glamore, W. C.; O'Carroll, D. M. A new framework for modeling the effect of salt on interfacial adsorption of PFAS in environmental systems. *Science of The Total Environment* **2021**, *796*, 148893.

(45) García, R. A.; Chiaia-Hernández, A. C.; Lara-Martin, P. A.; Loos, M.; Hollender, J.; Oetjen, K.; Higgins, C. P.; Field, J. A. Suspect screening of hydrocarbon surfactants in AFFFs and AFFF-contaminated groundwater by high-resolution mass spectrometry. *Environmental science & technology* **2019**, *53*, 8068–8077.

(46) Nickerson, A.; Maizel, A. C.; Kulkarni, P. R.; Adamson, D. T.; Kornuc, J. J.; Higgins, C. P. Enhanced extraction of AFFF-associated PFASs from source zone soils. *Environmental science & technology* **2020**, *54*, 4952–4962.

(47) Liu, M.; Munoz, G.; Vo Duy, S.; Sauvé, S.; Liu, J. Per-and polyfluoroalkyl substances in contaminated soil and groundwater at airports: a Canadian case study. *Environmental Science & Technology* **2021**, *56*, 885–895.

(48) Lucassen-Reynders, E. H. *Anionic surfactants: physical chemistry of surfactant action (pp. 1-51)*; Marcel Dekker, 1981; Vol. 11.

(49) Zhao, G.; Zhu, B.; Zhou, Y.; Shi, L. The surface-adsorption and micelle formation of the mixed aqueous-solutions of fluorocarbon and hydrocarbon surfactants. 2. Sodium perfluorooctanoate sodium decylsulfate system. *Acta Chimica Sinica* **1984**, *42*, 416–423.

(50) Vecitis, C.; Park, H.; Cheng, J.; Mader, B.; Hoffmann, M. Enhancement of perfluorooctanoate and perfluorooctanesulfonate activity at acoustic cavitation bubble interfaces. *The Journal of Physical Chemistry C* **2008**, *112*, 16850–16857.

(51) Brusseau, M. L.; Van Glubt, S. The influence of surfactant and solution composition on PFAS adsorption at fluid-fluid interfaces. *Water research* **2019**, *161*, 17–26.

(52) Silva, J. A.; Martin, W. A.; McCray, J. E. Air-water interfacial adsorption coefficients for PFAS when present as a multi-component mixture. *Journal of Contaminant Hydrology* **2021**, *236*, 103731.

(53) Ji, Y.; Yan, N.; Brusseau, M. L.; Guo, B.; Zheng, X.; Dai, M.; Liu, H.; Li, X. Impact of a hydrocarbon surfactant on the retention and transport of perfluorooctanoic acid in saturated and unsaturated porous media. *Environmental Science & Technology* **2021**, *55*, 10480–10490.

(54) Costanza, J.; Abriola, L. M.; Pennell, K. D. Aqueous film-forming foams exhibit greater interfacial activity than PFOA, PFOS, or FOSA. *Environmental Science & Technology* **2020**, *54*, 13590–13597.

(55) Huang, D.; Saleem, H.; Guo, B.; Brusseau, M. L. The impact of multiple-component PFAS solutions on fluid-fluid interfacial adsorption and transport of PFOS in unsaturated porous media. *Science of the Total Environment* **2022**, *806*, 150595.

(56) Kemball, C.; Rideal, E.; Guggenheim, E. Thermodynamics of monolayers. *Transactions of the Faraday Society* **1948**, *44*, 948–954.

(57) Broughton, D. Adsorption isotherms for binary gas mixtures. *Industrial & Engineering Chemistry* **1948**, *40*, 1506–1508.

(58) LeVan, M. D.; Vermeulen, T. Binary Langmuir and Freundlich isotherms for ideal adsorbed solutions. *The Journal of Physical Chemistry* **1981**, *85*, 3247–3250.

(59) Frey, D. D.; Rodrigues, A. E. Explicit calculation of multicomponent equilibria for ideal adsorbed solutions. *AIChE Journal (American Institute of Chemical Engineers);(United States)* **1994**, *40*.

(60) Lucassen-Reynders, E. A surface equation of state for mixed surfactant monolayers. *Journal of Colloid and Interface Science* **1972**, *41*, 156–167.

(61) Fainerman, V.; Lucassen-Reynders, E.; Miller, R. Adsorption of surfactants and proteins at fluid interfaces. *Colloids and Surfaces A: Physicochemical and Engineering Aspects* **1998**, *143*, 141–165.

(62) Mulqueen, M.; Blankschtein, D. Prediction of equilibrium surface tension and surface adsorption of aqueous surfactant mixtures containing ionic surfactants. *Langmuir* **1999**, *15*, 8832–8848.

(63) Fainerman, V.; Miller, R. Simple method to estimate surface tension of mixed surfactant solutions. *The Journal of Physical Chemistry B* **2001**, *105*, 11432–11438.

(64) Fainerman, V.; Miller, R.; Aksenenko, E. Simple model for prediction of surface tension of mixed surfactant solutions. *Advances in colloid and interface science* **2002**, *96*, 339–359.

(65) Fainerman, V.; Lucassen-Reynders, E. Adsorption of single and mixed ionic surfactants at fluid interfaces. *Advances in colloid and interface science* **2002**, *96*, 295–323.

(66) Pabon, M.; Corpart, J. Fluorinated surfactants: synthesis, properties, effluent treatment. *Journal of Fluorine Chemistry* **2002**, *114*, 149–156.

(67) Bagour, M. H. Measuring and predicting steady state infiltration rates for Arizona irrigated soils. 2001.

(68) Brusseau, M. L.; Peng, S.; Schnaar, G.; Murao, A. Measuring air- water interfacial areas with X-ray microtomography and interfacial partitioning tracer tests. *Environmental Science & Technology* **2007**, *41*, 1956–1961.

(69) Jiang, H.; Guo, B.; Brusseau, M. L. Characterization of the micro-scale surface roughness effect on immiscible fluids and interfacial areas in porous media using the measurements of interfacial partitioning tracer tests. *Advances in water resources* **2020**, *146*, 103789.

TOC Graphic

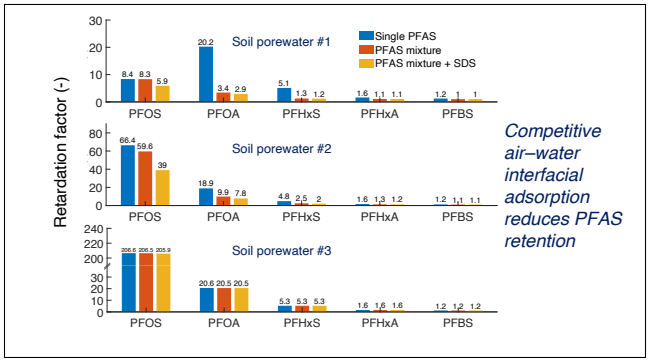
Retardation factor (-)
Soil porewater #1
Soil porewater #2
Soil porewater #3
Single PFAS
PFAS mixture
PFAS mixture + SDS
PFOS
PFOA
PFHxS
PFHxA
PFBS
Competitive air–water interfacial adsorption reduces PFAS retention